

Radiation Distribution Sensing With Normal Optical Fiber

R. Naka, K. Watanabe, J. Kawarabayashi, A. Uritani, T. Iguchi, N. Hayashi, N. Kojima, T. Yoshida, J. Kaneko, H. Takeuchi, and T. Kakuta

Abstract—The purpose of this study is to develop a radiation distribution monitor using a normal plastic optical fiber. The monitor has a long operating length and can obtain continuous radiation distributions. A principle of the position sensing is based on a time-of-flight technique. The monitor is sensitive to beta rays or charged particles, gamma rays, and fast neutrons. The spatial resolutions for beta-rays (^{90}Sr – ^{90}Y), gamma-rays (^{137}Cs), and D-T neutrons are 30, 37, and 13 cm, respectively. The detection efficiencies for the beta-rays, gamma-rays, and D-T neutrons are 0.11%, $1.6 \times 10^{-5}\%$ and $1.2 \times 10^{-4}\%$, respectively. The effective attenuation length of the detection efficiency is 18 m. In this paper, we describe the basic characteristics of this monitor.

I. INTRODUCTION

THERE is a demand for a new radiation distribution monitor that can be used around nuclear reactors, nuclear fusion experimental devices, accelerators, and so on. The monitor should have three characteristics, i.e., a long operation length, a continuous sensitivity, and real-time operation.

Recently, some methods [1] of radiation distribution sensing with optical fibers have been proposed. These methods employ a scintillating fiber [2], or scintillators with wavelength-shifting fibers [3]. In the former method, the attenuation length for the scintillation photons in the scintillating fiber is relatively short, so that the operating length of the sensor is limited to a few meters. In the latter method, the sensor cannot obtain a continuous radiation distribution but a discrete one.

To improve these shortcomings, we propose a new method using a normal plastic optical fiber (POF) made of polymethylmethacrylate (PMMA). The new radiation monitor has major advantages, such as a long operation length, continuous sensitivity, real-time operation, insensitivity to electromagnetic fields, and simple measuring system. We describe the characteristics of the radiation distribution monitor using the POF.

Manuscript received November 3, 2000; revised March 1, 2001. This work was supported in part by The JNC Cooperative Research Scheme on the Nuclear Fuel Cycle.

R. Naka, K. Watanabe, J. Kawarabayashi, A. Uritani, and T. Iguchi are with the Department of Nuclear Engineering, Nagoya University, 464-8603 Aichi, Japan (e-mail: naka@avocet.nucl.nagoya-u.ac.jp; kenichi@avocet.nucl.nagoya-u.ac.jp; okawa@cuckoo.nucl.nagoya-u.ac.jp; uritani@avocet.nucl.nagoya-u.ac.jp; iguchi@genius.nucl.nagoya-u.ac.jp).

N. Hayashi, N. Kojima, and T. Yoshida are with the Japan Nuclear Cycle Development Institute, 319-1194 Ibaraki-ken, Japan (e-mail: naomi@tokai.jnc.go.jp; nkojima@tokai.jnc.go.jp; yoshichu@tokai.jnc.go.jp).

J. Kaneko, H. Takeuchi, and T. Kakuta are with the Japan Atomic Energy Research Institute, 319-1195 Ibaraki, Japan (e-mail: kin@fnshp.tokai.jaeri.go.jp; takeuchi@fnshp.tokai.jaeri.go.jp; kakuta@stsp2a0.tokai.jaeri.go.jp).

Publisher Item Identifier S 0018-9499(01)10764-1.

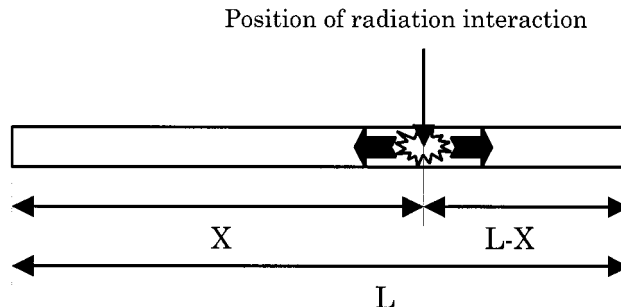


Fig. 1. Conceptual diagram of the position sensing method.

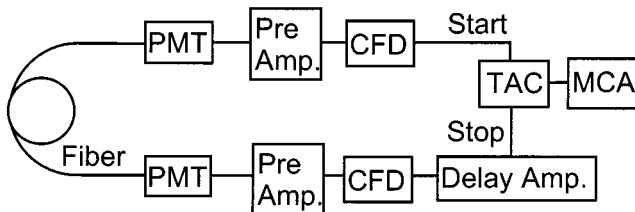


Fig. 2. The block diagram of the system.

II. PRINCIPLE AND SETUP

Fig. 1 shows the conceptual diagram of this position sensing method. The time-of-flight (TOF) technique was used to detect positions of radiation interactions. When a radiation enters and interacts with the POF, fluorescent and/or Cherenkov lights are emitted. When enough amounts of the photons are emitted within the critical angle of the POF and the photons reach both ends of the POF, the position of radiation interaction can be detected. When the photons reach both ends of the POF, we can obtain the following simple expression:

$$X - (L - X) = \frac{T_1 - T_2}{c'} \quad (1)$$

where X is the distance between the position of radiation interaction and the left end of the POF, c' is the velocity of light in PMMA, and T_1 and T_2 are time durations with which the photons reach the left and the right ends, respectively. Fig. 2 shows the block diagram of the measuring system. The length of the POF (Mitsubishi Rayon SH8001, Step index mode:multimode) was 10 to 100 m and the diameter was 2 mm. A photomultiplier tube (PMT; Hamamatsu-Photonics R1635) followed by a fast

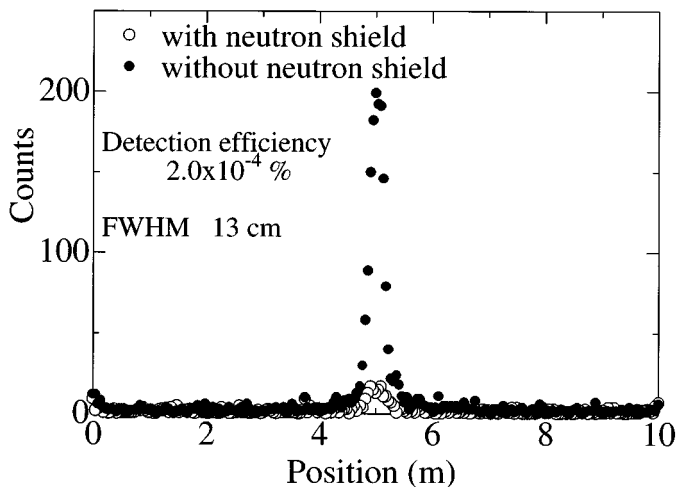


Fig. 3. The response to the D-T neutrons.

preamplifier (Ortec EG&G VT120) and a constant fraction discriminator (CFD) was connected to each end of the POF. The output signals of the POF were fed to a time-to-amplitude converter (TAC). The output pulse heights of the TAC were analyzed with a multichannel analyzer (MCA). A delay amplifier gave an appropriate delay time.

III. EXPERIMENTAL RESULTS

A. Response to Beta Rays

A ^{90}Sr - ^{90}Y beta source with an activity of 14 kBq was used. A cylindrical collimator with an inner diameter of 4.5 mm collimated the beta particles. The length of the POF was 10 m. The spatial resolution [full-width at half-maximum (FWHM)] was 30 cm. The intrinsic detection efficiency was 0.11%.

B. Response to Gamma Rays

A ^{137}Cs gamma-ray source with an activity of 54.2 MBq was used. A divergent collimator with inlet and outlet aperture diameters of 8 and 55 mm, respectively, and with a length of 40 mm was used. The POF was placed at the outlet aperture of the collimator. The length of the POF was 10 m. The spatial resolution was 37 cm. The intrinsic detection efficiency was $1.6 \times 10^{-5}\%$.

C. Response to Fission Neutrons

A fission neutron beam at the Yayoi [4] that was a fast neutron reactor was used. The neutron beam was collimated to 50 mm in diameter. The average energy was 1.3 MeV. The flux and the fluence were 4.5×10^6 n/cm²/s and 8.1×10^9 n/cm², respectively. The length of the POF was 10 m. The spatial resolution was 33 cm. The intrinsic detection efficiency was $2.0 \times 10^{-5}\%$.

D. Response to D-T Neutrons

A D-T neutron beam at the Fusion Neutronics Source [5] (FNS), Japan Atomic Energy Research Institute (JAERI), was used. The neutron beam was collimated to 20 mm in diameter. The length of the POF was 10 m. Fig. 3 shows the results of the neutron measurements with and without a polyethylene shield with a thickness of 40 cm that was placed in front

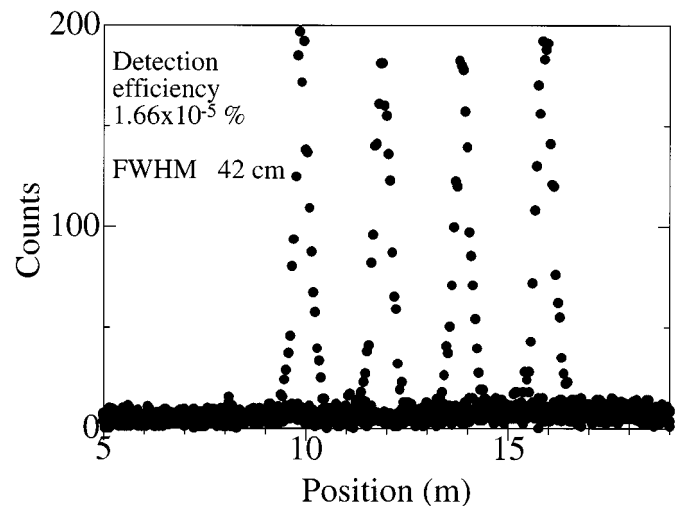


Fig. 4. The response to fast neutron at Yayoi (20-m fiber).

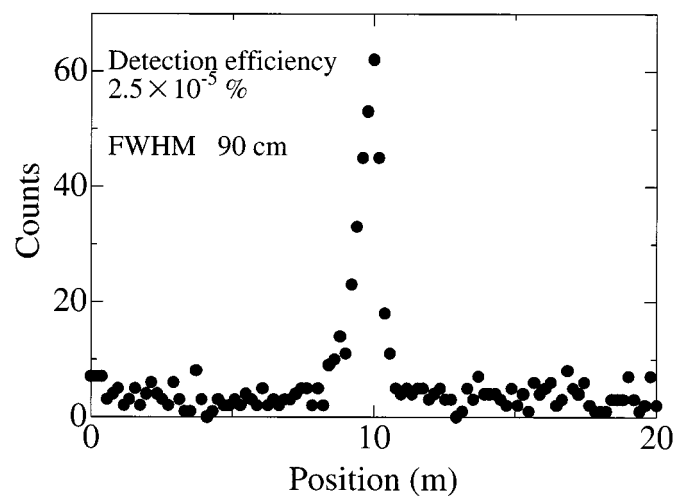


Fig. 5. The response to the D-T neutrons (50-m fiber).

of the POF. The flux was 1.2×10^6 n/cm²/s. The fluence was 7.2×10^8 n/cm². The spatial resolution was 13 cm. The intrinsic detection efficiency was $5.4 \times 10^{-4}\%$.

E. Measurements With Longer POFs

1) *Measurement With the 20-m POF:* The 20-m POF was used for the first step to develop a longer detector. The fission neutron beam at the Yayoi was used. The POF was irradiated by the neutrons at four different points to evaluate the position dependency of the detection efficiency and the spatial resolution. Fig. 4 shows the experimental results. The flux was 9.0×10^6 n/cm²/s. The fluence was 5.4×10^9 n/cm². The spatial resolution was 42 cm. The intrinsic detection efficiency was $1.7 \times 10^{-5}\%$. The intrinsic detection efficiency and the spatial resolution were worse than those obtained with the 10-m POF. No position dependency of these characteristics was observed. The ^{90}Sr - ^{90}Y beta source was also used. The spatial resolution was 46 cm. The intrinsic detection efficiency was $2.3 \times 10^{-4}\%$.

2) *Measurements With the 50-m POF:* The D-T neutron beam at the FNS was used. Fig. 5 shows the result obtained with the 50-m POF. The flux was 2.4×10^5 n/cm²/s. The

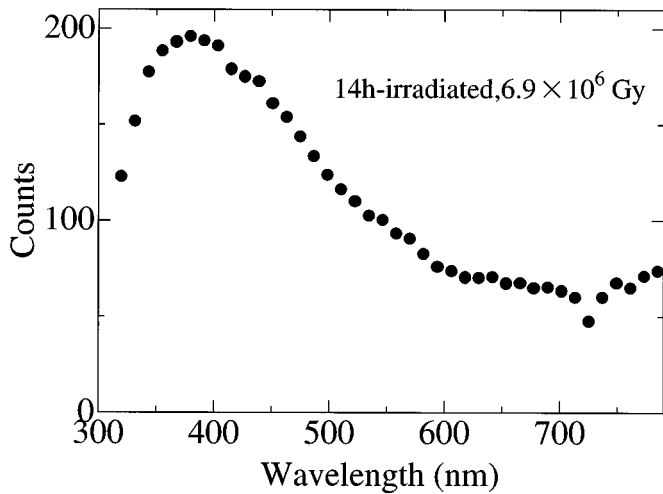


Fig. 6. The spectrum of the light emitted in jointed fiber.

fluence was 1.0×10^9 n/cm². The spatial resolution was 90 cm. The intrinsic detection efficiency was $2.5 \times 10^{-5}\%$.

3) *Measurements With the 100 m POF*: The D-T neutron beam at the FNS was used. The length of the POF was 100 m. The flux was 2.2×10^5 n/cm²/s. The fluence was 3.1×10^9 n/cm². The spatial resolution was 1.3 m. The intrinsic detection efficiency was $4.3 \times 10^{-6}\%$.

F. Optical Property of POF

We investigated the emission light spectrum at the ⁶⁰Co irradiation facility in JAERI to know the optical characteristics of the POF.

1) *Emission Spectrum*: A jointed fiber composed the POF with a length of 30 cm as an irradiation part and a quartz fiber as a transmission part was used. Fig. 6 shows the emission spectrum of the POF irradiated by ⁶⁰Co gamma-rays. The yield of Cherenkov photons per unit wavelength is proportional to $1/\lambda^2$. The emission is more intense in the short-wavelength region of the spectrum. The Cherenkov glow component was therefore dominant in the spectrum. However, the scintillating light existed in the wavelength region of 600 to 800 nm, and even in 400 to 600 nm region.

2) *Radiation Damage*: The emission spectra were measured to investigate radiation damages of the POF. Here both the irradiation and the transmission part are the POF. Fig. 7 shows the result. Some optical absorption by the POF existed before and after the irradiation. The absorptions at 530, 620, and 730 nm were due to the inherent optical absorption property of the POF. The light yield between 300 and 600 nm decreased by absorption due to radiation damage. The light components above 600 nm were not influenced by the irradiation.

G. Ratio of Foreground Events to Total Events

Only a small fraction of total scintillating events can be detected as the foreground events in this measurement because the small number of photons produced upon a radiation interaction cannot reach both ends of the POF due to the transmission property and a directional property of Cherenkov emission. We evaluated the fraction of the foreground events to the total one. The

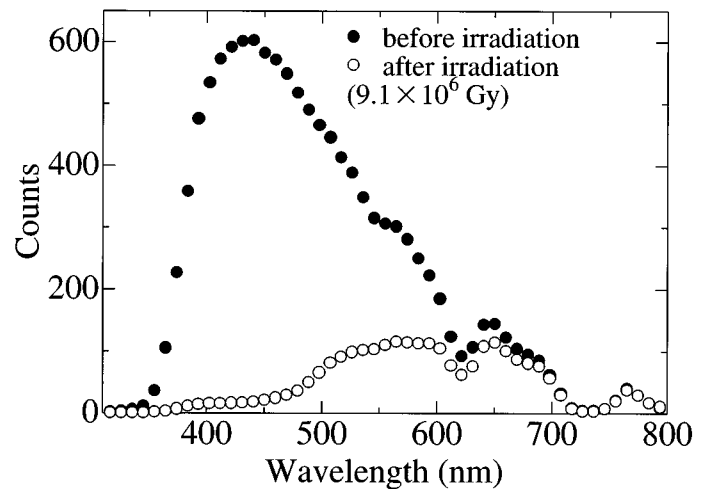


Fig. 7. The spectrum of the light emitted in the POF.

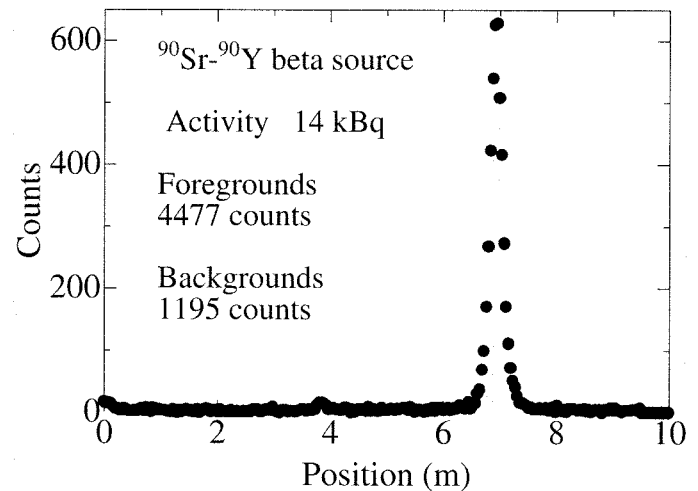


Fig. 8. The ratio of the foreground signals.

number of total events was obtained as the number of photons that reach the photocathode of the PMT when the ⁹⁰Sr-⁹⁰Y beta source is placed 5 cm from the PMT. The number of detected events as position signals, namely, foreground events, was obtained when the beta source was placed 7 m from the end of the POF with a length of 10 m. Fig. 8 shows the result. The fraction of the foreground to the total events was 0.4%. Most of the total events were the Cherenkov glows. Since Cherenkov photons had directional property, they seldom satisfy the detectable condition. Some of the backgrounds were chance coincidence events of the Cherenkov photons.

IV. DISCUSSION

A. Spatial Resolution

We calculated the expansion of a transmission time of photons by taking the mode dispersion of the POF into consideration. The fastest photons have no reflection during transmission before reaching the end of the POF, if the POF is straight. The slowest photons have much reflection during transmission along the path with the critical angle. The difference between

the fastest and the slowest accession times t is given by the following equations:

$$\tau = \left(\frac{n_1 \Delta}{c} \right) L \quad (2)$$

$$\Delta = \frac{n_1 - n_2}{n_1} \quad (3)$$

where n_1 and n_2 are the refractive indexes of the core (1.495) and the clad (1.402) and c is the velocity of light in vacuum. For example, we set one of the difference times as τ_1 and the other τ_2 . Since both sides of the POF are used, the maximum difference time is $\tau_1 + \tau_2$. When the 50-m POF was irradiated at 40-m point, the difference times τ_1 and τ_2 are 12 and 3 ns, respectively. The maximum difference time $\tau_1 + \tau_2$ is 15 ns, which corresponds to 1.4 m. As described before, the experimentally obtained FWHM and FWTM of the 50-m POF were 0.90 and 1.80 m, respectively. Therefore, the dominant factor that determines the spatial resolution is this time difference.

This detector has better spatial resolution for the D-T neutrons than for other radiations. In comparison with electrons, the energy deposited by a recoil proton is large. A 10-MeV recoil proton can deposit the full energy. On the other hand, a 1-MeV electron can deposit 400 keV at most. Approximately, the energy deposited is different about 30 times. Considering the yield of a light emission property of organic scintillators, the yield of the emission light by the recoil proton is roughly estimated to be about ten times larger than that by the electron. Since the large yield of the emission light for the D-T neutrons reduced fluctuations due to jitters and walks, the spatial resolution was relatively good.

B. Effective Attenuation Length for Detection Efficiency

When a radiation interacts with the POF and the photons are emitted at X in Fig. 1, the probability P_L that the photons reach the left end of the POF is expressed as $P_L = A \exp(-\mu X)$, where A is an appropriate constant value determined by the geometrical condition of the POF and m is the effective attenuation constant for the photons. Similarly, $P_R = A \exp[-\mu(L - X)]$. Hence the probability P that the photons reach both ends of the POF is expressed as

$$P = P_L P_R = A^2 \exp(-\mu L). \quad (4)$$

Therefore, the detection efficiency η depends on the length of the POF. We treated the μ as an effective attenuation constant value although it depends on the wavelength or the reflection angle. We measured the detection efficiency with the POF with four different lengths of 10, 20, 50, and 100 m to obtain the effective attenuation constant. The four detection efficiencies were fitted by the exponential function. Fig. 9 shows the graph of the detection efficiencies. The attenuation length $1/\mu$ of the POF was 18 m.

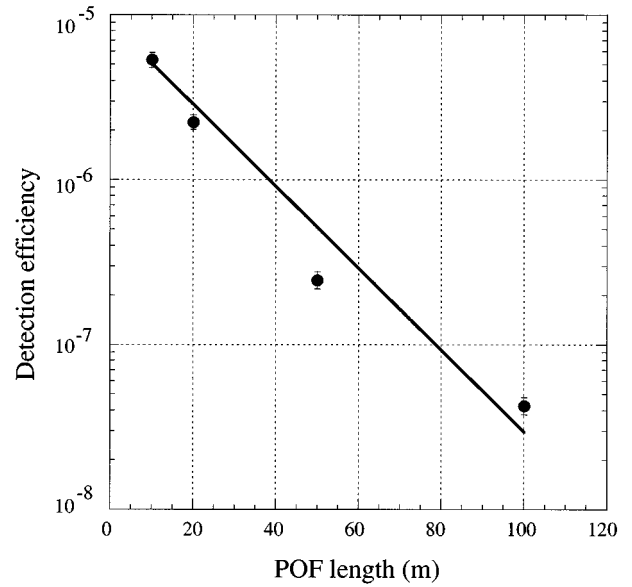


Fig. 9. The graph of the detection efficiencies to estimate the attenuation length.

C. Emission Spectrum

Since Cherenkov photons have the directional property, Cherenkov photons seldom satisfy the detectable condition. Therefore, the foreground signals were only 0.4% of the total event numbers. This detector can measure recoil protons produced by fast neutrons. We need to measure the wavelength spectrum of the emission light produced by the protons that are recoiled fast neutrons because D-T neutrons and the recoil protons never generate the Cherenkov photons.

V. CONCLUSION

We have developed a radiation distribution monitor using the POF for long, complicated, and narrow spaces. The responses of this monitor to the several radiations have been studied. We estimated the major factor of the spatial resolution. We obtained the effective attenuation length of the detection efficiencies.

REFERENCES

- [1] T. Kakuta, "Optical fibers and their applications for radiation measurements" (in Japanese), *Hoshasen*, vol. 24, no. 1, pp. 41–48, 1998.
- [2] T. Oka, H. Fujiwara, K. Takahashi, T. Usami, and Y. Tsutaka, "Development of fiber optic radiation monitor using plastic scintillation fibers," *J. Nucl. Sci. Technol.*, vol. 35, no. 12, pp. 857–864, 1998.
- [3] T. Maekawa, "Optical waveguide scintillator" (in Japanese), *Hoshasen*, vol. 21, no. 3, pp. 69–78, 1995.
- [4] S. Koshizuka *et al.*, "Research at the University of Tokyo fast neutron source reactor, YAYOI," JAERI-M-92-28, 1992.
- [5] C. Kutsukake, C. Kusano, J. Tanaka, and S. Abe, "Fusion neutronics. 14 MeV neutron generation characteristics of FNS tritium target (II). Beam energy dependency of neutron yield," JAERI-M-92-125, 1992.